Proceedings of the 11th International and 51st National Conference on Fluid Mechanics and Fluid Power (FMFP)
December 21-23, 2024, AMU Aligarh, Uttar Pradesh, India

FMFP2024-06-091

On the Acoustic Patterning of Droplets by Bessel Beams

Jeyapradhap Thirisangu[1], Videsh VK[1], Muthu Shravan Sundaram[1], and Karthick Subramani[1]

[1]Department of Mechanical Engineering, Indian Institute of Information Technology, Design and Manufacturing, Kancheepuram
*Corresponding Author, email: me21b1026@iiitdm.ac.in

ABSTRACT

In this work, we numerically investigate the flow pattern of mineral oil droplets within a circular well microchannel under the influence of standing acoustic waves. In the absence of acoustic forces, droplets move with the continuous fluid flow, travelling along the centre of the channel (where the velocity is higher). However, when the channel is subjected to acoustic waves, the droplets, having higher impedance, are drawn to the nearest nodes of the standing wave. The flow pattern of the droplets is primarily determined by the interplay between inertial forces and acoustic forces. When the acoustic force is dominant, droplets follow the circular path defined by the wave nodes. Conversely, if the inertial force is stronger, the droplets continue travelling along the centre of the channel with the continuous fluid flow. Additionally, we explored the impact of various parameters on droplet patterning, including the frequency of the acoustic waves, the inlet velocity of the fluid, and the acoustic energy density. These factors significantly influence the positioning and movement of the droplets within the microchannel.

I. INTRODUCTION

The field of study involving the introduction of acoustic fields into a microchannel containing inhomogeneous fluids has been extensively studied and is called 'microscale acoustofluidics'. The analysis of fluid behaviour in channels or cavities with dimensions of the order of tens and hundreds of micrometres displays certain interesting phenomena which have been extensively studied in the past. The popularity of miniaturisation has led to the development of the field of 'droplet microfluidics', especially a branch known as 'segmented flow microfluidics', which deals with droplets dispersed in an immiscible carrier fluid. Water-in-oil droplets are often used because of their potential in experimental biology. The predominantly investigated acoustic phenomena involve the acoustic radiation force and acoustic streaming. These investigations have a long history, with early investigations being conducted by Faraday,[9] Rayleigh,[12] King,[13] and Lighthill.[8] There has been a growing interest in microfluidic applications in light of recent developments and their significance in the chemical, biomedical, and healthcare industries[11,4,10].

In mini-scale acousto-fluidic systems, the actuation methods frequently used are acoustic ration force and acoustic streaming. To manipulate the droplets in these segmented flow studies, the acoustic radiation force was developed. In 1934, King[13] conducted a detailed theoretical study to explain the effects of acoustics on a small rigid sphere, providing an expression for the radiation pressure exerted, initially neglecting compressibility. It was Gor'kov[3] who later formulated the acoustic radiation force as the gradient of a potential (now known as the Gor'kov potential), which depends on the time-averaged kinetic and potential energies of the acoustic fields.

The acoustic radiation force developed as a result of the applied standing acoustic waves drives the droplets or particles towards the acoustic pressure nodes or antinodes, depending on the mechanical properties of the dispersed medium. In this work, we actuate a circular well, resulting in Bessel beams producing the acoustic radiation force, to study the role of the interplay between inertial forces and acoustic forces on the behaviour of an acoustically hard water droplet dispersed in a free-flowing continuous medium of mineral oil.

II. METHODOLOGY

When the circular well is actuated with acoustic waves of a specified wavelength, the pressure nodes and anti-nodes are formed as concentric regions, centered at the circular well. The channel that is implemented in our study is illustrated in Fig. 2. Pressure antinodes arise from the crests and troughs of the Bessel function, representing maxima and minima, respectively, while nodes correspond to points where the Bessel function equals zero.

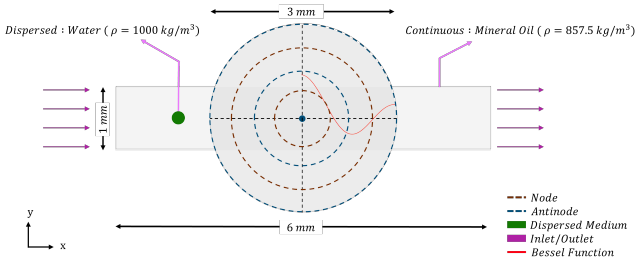

Figure 1: A 2D illustration of a channel containing a circular well, with two acoustic pressure nodes and three antinodes forming as concentric rings around the centre as a result of the Bessel beam. The green dot highlights the initial location of the dispersed water droplet in a continuous medium of mineral oil.

The governing equations of hydrodynamics in acoustofluidic systems include mass-continuity, momentum and advection-diffusion equations, and the thermodynamic pressure-density relation as given below,[7]

$$\partial_t \rho + \nabla \cdot (\rho \boldsymbol{v}) = 0, \tag{1a}$$

$$\rho[\partial_t \boldsymbol{v} + (\boldsymbol{v} \cdot \nabla)\boldsymbol{v}] = -\nabla p + \eta \nabla^2 \boldsymbol{v} + \beta \eta \nabla(\nabla \cdot \boldsymbol{v}) + \rho \boldsymbol{g}, \tag{1b}$$

$$\partial_t s + \boldsymbol{v} \cdot \nabla s = D \nabla^2 s, \tag{1c}$$

where ρ is the density, $\boldsymbol{v}$ is the velocity, p is the pressure, η is the dynamic viscosity of the fluid, ξ is the bulk viscosity, $\beta = (\xi/\eta) + (1/3)$, $\boldsymbol{g}$ is the acceleration due to gravity in the negative y-direction, s is the solute concentration and D is diffusivity. We require following thermodynamic pressure-density relation in terms of material derivative[1] $(d/dt) = \partial_t + (\boldsymbol{v} \cdot \nabla)$ as well,

$$\frac{d\rho}{dt} = \frac{1}{c^2}\frac{dp}{dt}, \tag{1d}$$

where $c^2 = (\partial p/\partial \rho)|_S$ and c is the adiabatic local speed of sound. The fluid flow is assumed to be laminar and isothermal and the gravitational body force is neglected as it has negligible effects as compared to the acoustic force density. When the microchannel containing fluid is actuated by acoustic fields of frequency ($\sim$ 1 MHz),. The physics involved in a fluid containing microchannel, actuated by acoustic fields, has two separate time scales, i.e., fast scale acoustics ($t_f \sim 0.1$ μs) and the slow scale hydrodynamics ($\tau \sim 10$ ms).[6] The second-order fields can capture the slow time-scale acoustic phenomena such as acoustic streaming, acoustic relocation and acoustic radiation. The divergence of the Reynolds stress tensor results in the acoustic body force responsible for the second-order slow hydrodynamic flows, as given below,

$$\boldsymbol{f}_{ac} = -\nabla \cdot \langle \rho_0 \boldsymbol{v}_1 \boldsymbol{v}_1 \rangle. \tag{2}$$

Upon decomposing this equation, we obtain:

$$\begin{aligned} f_{ac} = &\frac{1}{2}\nabla\left(\kappa_0 \left\langle |p_1|^2 \right\rangle - \rho_0 \left\langle |v_1|^2 \right\rangle\right) + \\ &\langle v_1 \times \nabla \times (\rho_0 v_1) \rangle - \\ &\frac{1}{2}\left[\left\langle |p_1|^2 \right\rangle \nabla \kappa_0 + \left\langle |v_1|^2 \right\rangle \nabla \rho_0\right]. \end{aligned} \tag{3}$$

where the first term only contributes to the second-order pressure and does not contribute to Acoustic Relocation. Similarly, the second term only contributes to Acoustic Streaming. Thus, we neglect these terms and consider only the third term,

$$-\frac{1}{2}\left[\left\langle |p_1|^2 \right\rangle \nabla \kappa_0 + \left\langle |v_1|^2 \right\rangle \nabla \rho_0\right], \tag{4}$$

which is responsible for relocating the fluid. By taking the time average of the above term, we obtain

$$f_{ac} = -\frac{1}{4}|p_1|^2 \nabla \kappa_0 - \frac{1}{4}|v_1|^2 \nabla \rho_0, \tag{5}$$

where p_1 denotes the first-order acoustic pressure, v_1 shows the velocity fields, κ_0 and ρ_0 denote the zeroth-order compressibility and density of the fluid respectively. The compressibility (κ_0) is expressed in terms of the density of the fluid (ρ_0) and the speed of sound in the fluid (c) as

$$\nabla \kappa_0 = \nabla\left(\frac{1}{\rho_0 c_0^2}\right) = -\kappa_0 \frac{\nabla \rho_0}{\rho_0} - 2\kappa_0 \frac{\nabla c_0}{c_0}. \tag{6}$$

Substituting in Eq. 5, we get

$$f_{\text{ac}} = \frac{1}{4}\left[\kappa_0 |p_1|^2 - \rho_0 |v_1|^2\right]\frac{\nabla \rho_0}{\rho_0} + \frac{1}{2}\kappa_0 |p_1|^2 \frac{\nabla c_0}{c_0}. \tag{7}$$

In the weakly inhomogeneous limit, where the variations in density ρ_0 and speed of sound c_0 are small, the first-order pressure and velocity fields, as described by Karlsen et al.,[6] can be expressed as

$$p_1 = p_a \hat{p}_1 e^{-i\omega t}, \quad v_1 = \frac{-i p_a}{k_0 c_0 \rho_0}\nabla \hat{p}_1 e^{-i\omega t}, \tag{8}$$

where p_a denotes the acoustic pressure amplitude, ω is the acoustic angular frequency, k_0 is the wave number and $\hat{p}_1^{(0)}$ is the non-dimensionalized pressure field. Substituting Eq. 8 in Eq. 7, we get:

$$f_{\text{ac}} = E_{\text{ac}}[(|\hat{p}_1|^2 - (k_0)^{-2}|\nabla \hat{p}_1|^2)\nabla \hat{\rho} + (2|\hat{p}_1|^2)\nabla \hat{c}]. \tag{9}$$

We implement the Bessel function pressure field, given by Courtney et al.(2013),[2]

$$\hat{p}_1 = J_l(k_0 r)\, e^{il\theta}, \tag{10}$$

where J_l is the l^{th} order Bessel function of the first kind and r is the radial distance. Rewriting Eq. 9 in terms of Eq. 10 and using the relations, $2J_l'(\hat{r}) = J_{l-1}(\hat{r}) - J_{l+1}(\hat{r})$ and $(2l/r)J_l(\hat{r}) = J_{l-1}(\hat{r}) + J_{l+1}(\hat{r})$ we get:

$$\begin{aligned} f_{\text{ac}} = E_{\text{ac}}[&([J_l(\hat{r})]^2 - \frac{1}{2}[J_{l-1}(\hat{r})]^2) \\ &-\frac{1}{2}[J_{l+1}(\hat{r})]^2 \nabla \hat{\rho} + (2[J_0(\hat{r})]^2)\nabla \hat{c}] \end{aligned} \tag{11}$$

In this study, we are using a zeroth-order Bessel function of the first kind, and hence substituting it into Eq.11 using the relations specified above. we get:

$$f_{\text{ac}} = E_{\text{ac}}[([J_0(\hat{r})]^2 - [J_1(\hat{r})]^2)\nabla \hat{\rho} + (2[J_0(\hat{r})]^2)\nabla \hat{c}] \tag{12}$$

This study examines a single inlet circular well flow configuration frequently utilized in experiments in the domain of acoustofluidics as shown in Fig.2. By simplifying this 3D problem into a 2D representation focused solely on the x-y plane, we can accurately capture all pertinent physical phenomena while significantly reducing computational demands and time requirements. Furthermore, several prior theoretical acoustofluidic studies have taken this simplified 2D approach, making our assumptions valid.

The circular well configuration was numerically simulated using COMSOL Multiphysics 6.2 involving a two-phase flow model with bidirectional coupling, where mineral oil serves as the continuous medium and De-Ionized (DI)

Table 1: Properties of the phases employed in this study. CM denotes the continuous medium (fluid) and DM denotes the dispersed medium (droplet).

Medium	CM	DM
Density (ρ) $[kg/m^3]$	857.5	1000
Speed of sound (c) $[m/s]$	1440	1496.3
Dynamic Viscosity (μ) $[Pa.s]$	27.5e-3	1e-3
Surface Tension $[N/m]$	5×10^{-3}	

water as the dispersed medium. The Level-Set method is employed to differentiate the phases and define the water droplets within the mineral oil. A Bessel beam is introduced inside a circular channel, with its wavelength matching the channel radius, resulting in a single full-length wave of $\lambda = 1.5\ mm$. The fluid's inlet velocity is set at $0.001\ m/s$. As a result of the applied Bessel beam, The relevant properties of the mineral oil and DI water are provided in Table 1. This setup allows for the detailed investigation of droplet behaviour under the influence of the Bessel beam within the channel.

A. Validation

The numerical analysis was carried out using a grid with $18,708$ triangular grid elements, with a maximum element size of 39 μm and minimum element size of $4.5 \times 10^{-4}\ mm$ which was chosen as a trade-off between processing time and precision. The mesh chosen was validated by a grid independence test of the fluid velocity at the centre of the circular well, as shown below.

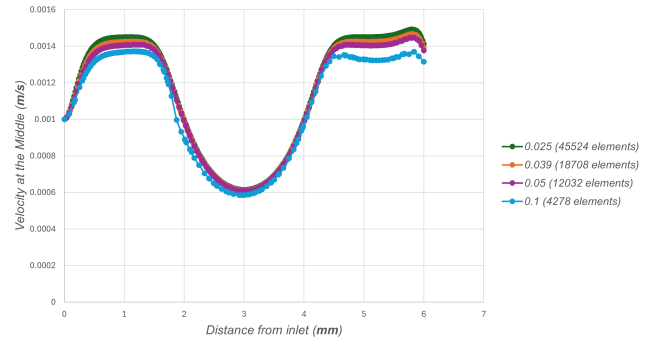

Figure 2: A comparison of the fluid velocity at the centre of the circular well, to validate the mesh chosen.

The behaviour of the acoustically "hard" droplets (meaning that they have a positive (+ve) Contrast Factor) is as predicted by the acoustic body force given above. The results are coherent with the acoustic patterning observed by Karlsen et al.(2017).[5]

III. RESULTS AND DISCUSSION

The behaviour of a single droplet dispersed in water, as shown in Fig.2, has been studied here. This study includes configurations with varied levels of applied acoustic energy density (E_{ac}), to study the effects of acoustics on the dynamics experienced by the droplet. The physical phenomena experienced by the droplet as a result of dispersion in a fluid located in a circular well are discussed in detail below.

A. Without any acoustics ($E_{ac} = 0$)

We initially examine a scenario without the application of acoustic waves. When the fluid is allowed to flow through the channel described by Fig.2 with an inlet velocity of $v = 0.001\ m/s$, the droplet begins to move along the flow of the fluid.

This behaviour is primarily due to the momentum imparted to the droplet by the inertial and viscous forces from the fluid flow. As the fluid and droplet enter the circular channel, the fluid velocity is highest along the centerline of the circle, while it significantly decreases near the boundary of the channel. Consequently, the droplet is carried along the central flow path, avoiding deviation towards the channel walls. This central flow ensures the droplet remains away from the boundaries and continues its journey through the channel, eventually moving towards the outlet. The droplet residence time, which indicates the duration the droplet remains within the circular channel, is $\approx$ 3.6 s, as observed from Fig.3.

B. Upon actuation with acoustics ($E_{ac} \neq 0$)

Now, we investigate the behaviour of an acoustically hard droplet when the circular well is actuated with acoustic waves in the form of Bessel beams. In this configuration, the channel containing the circular well is actuated with beams of wavelength $\lambda = 1.5\ mm$, which matches the radius of the circular well. This setup creates a pattern of acoustic pressure nodes and antinodes as concentric circles centred around the well. Due to the droplet's properties, it behaves as an acoustically hard object, characterized by a positive contrast factor, causing it to be attracted towards the pressure nodes.

When the fluid is allowed to flow through the channel described by Fig.2 with an inlet velocity of $v = 0.001\ m/s$, the droplet begins to move along with the flow of the fluid, primarily due to the inertial and viscous force effects from the fluid flow. When the droplet and the fluid enter the circular channel, which has a standing acoustic wave in the form of a vessel function, the fluid flows normally, with a higher velocity at the centerline of the circle and a lower velocity near the boundaries of the circle. The fluid does not exhibit acoustic phenomena such as acoustic relocation by the acoustic wave applied, primarily as the domain consists of a single homogeneous fluid. Whereas, the acoustically hard droplet is directed towards the pressure nodes by the acoustic force. The behaviour of the droplet as it moves towards the node varies with the level of the energy density (E_{ac}) of the acoustic force.

1) $E_{ac} = 10\ J/m^3$: When actuated with a Bessel beam of $E_{ac} = 10\ J/m^3$, the effect of the acoustic force is weak, when compared with the inertial and viscous effects of the fluid on the droplet. As a result, the acoustically hard droplet follows almost the same trajectory exhibited by the

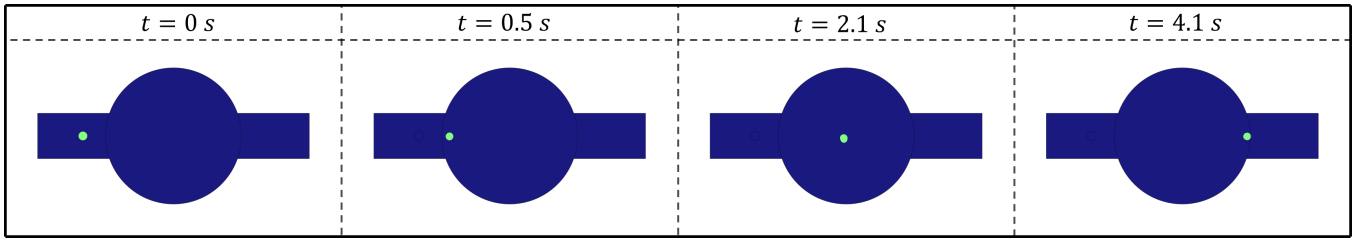

Figure 3: **Configuration of the channel without applied acoustics, showing droplet movement driven solely by the inertial forces of the moving fluid. The dispersed medium (droplet) is represented by the green circle while the dark blue area represents the continuous medium (fluid).**

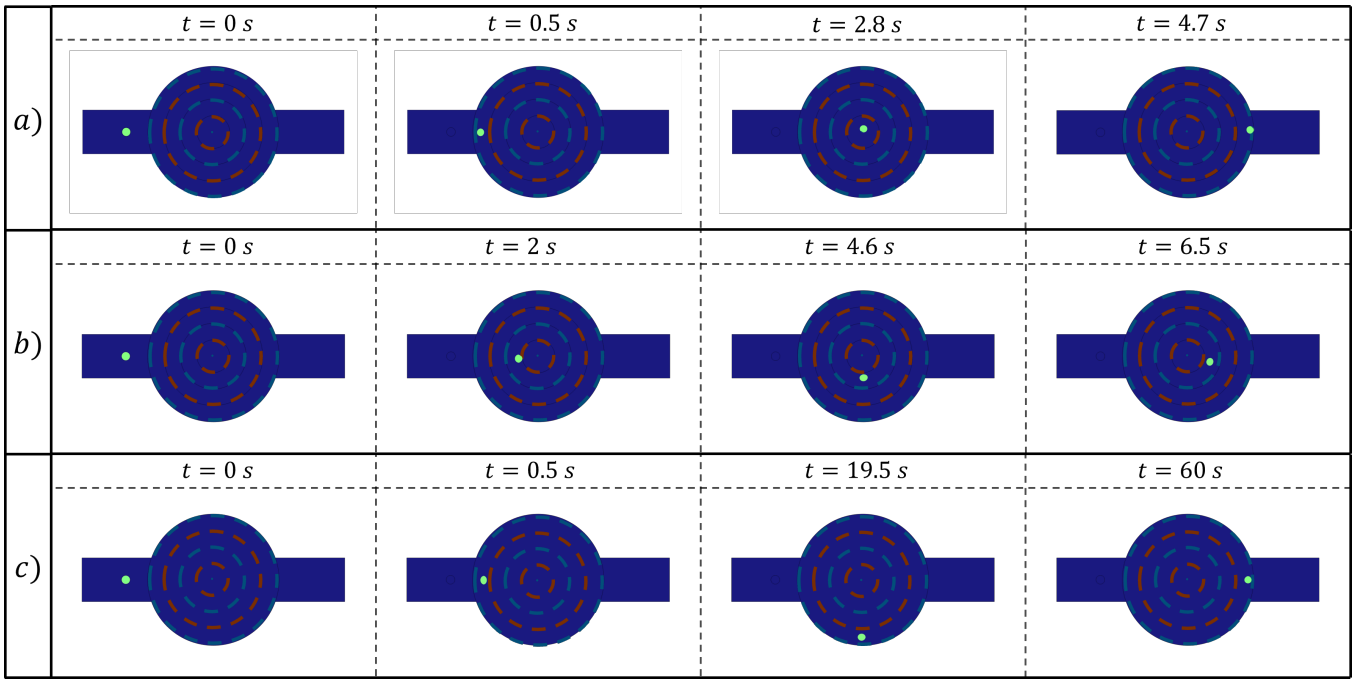

Figure 4: **Various configurations of the channel with applied acoustics at energy densities of a)** $E_{ac} = 10\ J/m^3$**, b)** $E_{ac} = 100\ J/m^3$ **and c)** $E_{ac} = 400\ J/m^3$**. The red dotted lines indicate pressure nodes, the blue dotted lines indicate antinodes and the dispersed medium (droplet) is represented by the green circle. The dark blue area represents the continuous medium (fluid). The droplet's movement is influenced by the combined effects of acoustic, inertial, and viscous forces**

droplet when no acoustics are applied, as evident in Fig.4.a). However, when the droplet approaches the nodal region near the centre of the circular well, it does experience a slight deviation from it's initial trajectory, which is highlighted in Fig.4.a) at time $t = 2.8\ s$. The droplet appears to be closer to the top of the inner circular node than the centre of the circular well. Although the droplet experiences a slight deviation, it ultimately progresses towards the outlet of the channel. Interestingly, the droplet residence time has increased and appears to be $\approx\ 4.2\ s$. This increase in residence time is attributed to the acoustic effects induced in the channel. The acoustically hard droplet is drawn towards the nodes, increasing the resistance to flow along with the fluid.

2) $E_{ac} = 100\ J/m^3$*:* When actuated with a Bessel beam of $E_{ac} = 100\ J/m^3$, the effect of the acoustic force is stronger and is comparable to the inertial and viscous effects of the fluid on the droplet. When the droplet enters the circular well, initially, the inertial force appears to dominate over the acoustic effects, resulting in the motion of the droplet along the centerline of the circle. However, when the droplet approaches the nodal region near the centre of the circular well, the acoustic force has a much higher effect on the droplet than the inertial force. As a result, the droplet is forced to travel along the innermost pressure node, following a circular trajectory, which is highlighted in Fig.4.b) at time $t = 4.6\ s$. Despite the presence of inertial and viscous effects, which

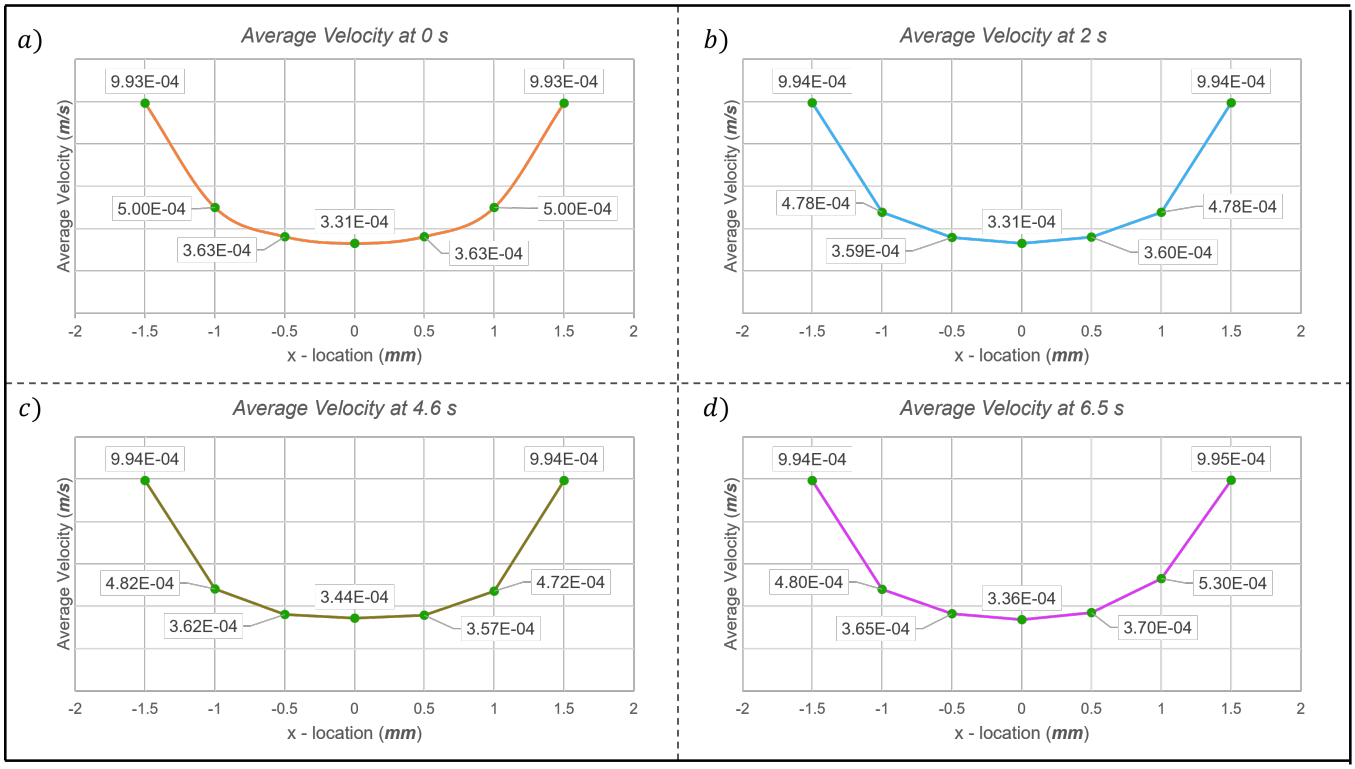

Figure 5: **Velocity profiles plotted at different offsets from the center of the circular well for the configuration where acoustics is applied with an energy density of $E_{ac} = 100\ J/m^3$. The profiles are plotted for different time steps of the progression.**

are unable to overpower the acoustic force, these effects still influence the droplet's motion. Consequently, the droplet does not precisely align with the node, instead travels at a slight offset. Remarkably, as the droplet proceeds towards the far end of the node, closest to the outlet, the droplet slows down and ultimately becomes stationary at the same point, as shown in Fig.4.b) at time $t = 6.5\ s$. The droplet does not move beyond this point and does not progress to the outlet of the channel. The droplet becomes stationary as the acoustic and inertial forces acting on the droplet balance each other out, and provide a region of effectively no force. The droplet slows down due to the viscous effects exhibited by the fluid. This configuration is particularly valuable as it presents a novel method for trapping or isolating droplets, or groups of droplets, with specific sizes and properties from a mixture of inhomogeneous droplets and fluids.

3) $E_{ac} = 400\ J/m^3$*:* When actuated with a Bessel beam of $E_{ac} = 400\ J/m^3$, the effect of the acoustic force is much stronger than the inertial and viscous effects of the fluid on the droplet. Consequently, the droplet is driven along the outermost pressure node, following a circular trajectory larger than the previous case, as highlighted in Fig.4.c) at time $t = 19.5\ s$. The progression of the droplet along the pressure node is due to the inertial force exerted by the fluid. However, due to the significantly reduced fluid velocity near the boundary of the circular well compared to the centerline, the inertial forces in this region are markedly weaker than at the inlet or outlet of the channel. Consequently, the droplet's progression is substantially slower, resulting in an extended time to reach the end of the node near the channel outlet. The droplet ultimately progresses towards the outlet, as show in Fig.4.c). Comparing the time taken for the droplet to progress towards the outlet in this configuration with the previous cases, it is observed that the time is approximately an order of magnitude higher than the time taken previously

C. Study of velocity profiles

The average fluid velocity along the length of the Bessel channel at multiple time steps exhibits distinct variations, as depicted in Fig.5. Initially, without the influence of acoustics, the velocity is highest at the inlet of the channel, as evident from the initial and final points in all time steps from Fig.5. This can be attributed to the smaller cross-sectional area at the inlet, which accelerates the flow. As the fluid progresses along the channel, the average velocity decreases due to the increasing diameter of the channel, which results in a larger cross-sectional area and consequently a reduction in velocity to maintain a constant flow rate. This decrease in velocity continues until the midpoint of the channel, where the diameter is at its maximum. Beyond this midpoint, the average velocity begins to increase again as the channel diameter decreases towards the outlet. Ultimately, the velocity reaches its peak at the end of the Bessel channel due to

the narrowing cross-sectional area that accelerates the fluid flow once more. Correspondingly, the inertial force is at its maximum at the start of the channel, decreases until the midpoint, and then begins to increase again, reaching its maximum at the end of the channel. Consequently, the water droplet in the continuous medium is driven by this varying inertial force and moves along the channel, following the described velocity profile.

In the presence of the acoustic force, the droplet motion depends on the interplay between the acoustic and inertial forces. The acoustic force is applied in such a way that two nodes are formed in a circular pattern within the Bessel channel, as shown in Fig.2. For a stable condition, when the fluids are subjected to acoustics, the water droplet migrates to the nodes. The resulting motion or trajectory of the droplet in the Bessel channel is determined by the balance between the acoustic and inertial forces. If the applied acoustic force is strong enough to overcome the inertial force, the droplet follows the trajectory of the first node, as depicted in Fig.4. However, if the acoustic force is just strong enough to slightly surpass the inertial force, the droplet may not follow the first node path, where the inertial force is high. Instead, it will follow the second node path, where the inertial force is comparatively lower, allowing the acoustic force to dominate. This scenario is illustrated in Fig.4.b). If the inertial force is dominant over the acoustic force, the droplet moves in a straight path, similar to the case without acoustics. The only difference in this scenario is that the residence time of the droplet in the channel increases due to the influence of the acoustic force, as shown in Fig.3 and Fig.4.

IV. CONCLUSIONS

In this study, we numerically investigated the flow patterns of mineral oil droplets within a circular well microchannel under the influence of standing acoustic waves. Our findings highlight the significant role of the interplay between inertial forces and acoustic forces in determining droplet behaviour. Without acoustic forces, droplets travel along the centre of the channel with the continuous fluid flow. However, the application of standing acoustic waves causes droplets to move towards the nearest nodes due to their higher impedance.

The study further reveals that the dominance of acoustic forces leads to droplets following the circular paths of the wave nodes, while stronger inertial forces cause droplets to maintain their central trajectory. Additionally, our exploration of various parameters, such as the frequency of acoustic waves, inlet fluid velocity, and acoustic energy density, underscores their critical impact on droplet patterning.

These insights contribute to a deeper understanding of droplet manipulation within microchannels and can inform the design and optimization of acoustofluidic devices for various applications, including lab-on-a-chip technologies and biomedical diagnostics.

ACKNOWLEDGEMENTS

We acknowledge the support and resources provided by the Indian Institute of Information Technology, Design and Manufacturing (IIITDM) Kancheepuram. Their facilities and environment have been instrumental in the completion of this work.

NOMENCLATURE

E_{ac}	Acoustic Energy Density	$[J/m^3]$
v	Velocity	$[m/s]$
λ	Wavelength	$[mm]$

REFERENCES

[1] Peter G. Bergmann, *The Wave Equation in a Medium with a Variable Index of Refraction*, J. Acoust. Soc. Am. **17** (2005), no. 4, 329.

[2] Charles R. P. Courtney, Bruce W. Drinkwater, Christine E. M. Demore, Sandy Cochran, Alon Grinenko, and Paul D. Wilcox, *Dexterous manipulation of microparticles using Bessel-function acoustic pressure fields*, Appl. Phys. Lett. **102** (2013), no. 12.

[3] L. P. Gor'kov, *On the Forces Acting on a Small Particle in an Acoustical Field in an Ideal Fluid*, Soviet Physics Doklady **6** (1962), 773.

[4] Gi Seok Jeong, Seok Chung, Chang-Beom Kim, and Sang-Hoon Lee, *Applications of micromixing technology*, Analyst **135** (2010), no. 3, 460–473.

[5] Jonas T. Karlsen and Henrik Bruus, *Acoustic Tweezing and Patterning of Concentration Fields in Microfluidics*, Phys. Rev. Appl. **7** (2017), no. 3, 034017.

[6] T. Karlsen, P. Augustsson, and H. Bruus, *Acoustic force density acting on inhomogeneous fluids in acoustic fields*, Phys. Rev. Lett. **117** (2016), no. 11, 114502.

[7] L. D. Landau and E. M. Lifshitz, *Fluid Mechanics*, Pergamon, Oxford, England, UK, Aug 1987.

[8] Sir James Lighthill, *Acoustic streaming*, J. Sound Vib. **61** (1978), no. 3, 391–418.

[9] Faraday Michael, *XVII. On a peculiar class of acoustical figures; and on certain forms assumed by groups of particles upon vibrating elastic surfaces*, Philos. Trans. R. Soc. Lond. **121** (1831), 299–340.

[10] Yiming Mo, Girish Rughoobur, Anirudh M. K. Nambiar, Kara Zhang, and Klavs F. Jensen, *A Multifunctional Microfluidic Platform for High-Throughput Experimentation of Electroorganic Chemistry*, Angew. Chem. Int. Ed. **59** (2020), no. 47, 20890–20894.

[11] Seyed Ali Nabavi, Goran T. Vladisavljević, and Vasilije Manović, *Mechanisms and control of single-step microfluidic generation of multi-core double emulsion droplets*, Chem. Eng. J. **322** (2017).

[12] Lord Rayleigh, *On the Circulation of Air Observed in Kundt's Tubes, and on Some Allied Acoustical Problems*, Philos. Trans. R. Soc. Lond. **175** (1884), 1–21.

[13] King Louis Vessot, *On the acoustic radiation pressure on spheres*, Proc. R. Soc. London A - Math. Phys. Sci. **147** (1934), no. 861, 212–240.